

AperTO - Archivio Istituzionale Open Access dell'Università di Torino

A new application of Curvatool semi-automatic approach to qualitatively detect geological lineaments

This is a pre print version of the following article:

Original Citation:

Availability:

This version is available <http://hdl.handle.net/2318/1647552> since 2018-06-19T16:18:19Z

Published version:

DOI:10.2113/gseegeosci.23.3.179

Terms of use:

Open Access

Anyone can freely access the full text of works made available as "Open Access". Works made available under a Creative Commons license can be used according to the terms and conditions of said license. Use of all other works requires consent of the right holder (author or publisher) if not exempted from copyright protection by the applicable law.

(Article begins on next page)

1 **A new application of CurvaTool semi-automatic approach to qualitatively detect**
2 **geological lineaments**

3 ***Bonetto Sabrina^a, Facello Anna^b, Umili Gessica^a**

4 ^a Department of Earth Sciences, University of Turin, Valperga Caluso 35, 10125 Turin,
5 Italy. {sabrina.bonetto, gessica.umili}@unito.it; 00390116705139

6 ^b CNR-IRPI, Strada delle Cacce,73 - 10135 Torino, Italy. anna.facello@irpi.cnr.it

7 *Corresponding author: Sabrina Bonetto, Department of Earth Sciences, University of Turin,
8 Valperga Caluso 35, 10125 Turin, Italy. sabrina.bonetto@unito.it; 00390116705139

9 **Abstract**

10 In the ^{past} last few years, lineament analysis ^{has become} is an important analytical technique for delineation of
11 major structural units in mineral prospecting, hydrogeology, and tectonic studies. The use of
12 remote sensing, with progressive development of image enhancement techniques, provides an
13 opportunity to produce more reliable and comprehensive lineament maps. In this paper, we
14 propose the application of a semi-automatic approach based on Digital Terrain Models
15 (DTM) for the extraction of potential lineaments and their detailed validation. ^{info selected} An area
16 belonging to the Bagni di Vinadio municipality (Cuneo, NW Italy), which is part of the
17 Argentera Massif (Western Alps), ^{is} was selected as a test site. Data obtained from the code
18 CurvaTool, developed by the authors, are successfully compared with literature information
19 and with lineaments obtained from visual interpretation of remote sensing imagery.
20 CurvaTool code permits the extraction and classification of a greater number of linear features
21 ^{compared} with respect to visual interpretation techniques. The ability to detect features that are not
22 perceptible by visual observation is a strong point ^{of} for CurvaTool processing. In the test area,
23 CurvaTool output data correlate with visually detected linear features and show a good
24 correlation with regional tectonics and iso-kinematic maps from ^{the} literature.

25 **Keywords:** Geological structure, Lineament extraction, DTM, Semi-Automatic survey,
26 Argentera Massif

27

28

29

30 1 - INTRODUCTION

31 Detection and extraction of lineaments ^{are} is an important step^s in analyses related to mineral
32 prospecting, hydrogeology studies, ^{and} and tectonic studies to delineate major structural units,
33 analyze structural deformation patterns, and identify geological boundaries (Clark and
34 Wilson, 1994; Davis and Reynolds 1996; Rangzan et al., 2008; Lee et al., 2012). Usually,
35 lineament maps created by field works ^{cannot} identify all the lineaments that exist in an area,
36 due to the limited point of view of the mapper with respect to the geological structures. Field
37 work can be a time consuming, expensive and sometimes a dangerous undertaking. Therefore,
38 any technique that can make field work more efficient is thus beneficial.

39 In the past few years the use of remote sensing products, coupled with progressive
40 development of image enhancement techniques, has provided scientists with a fast and
41 relatively cheap way to gather information that complements classical field geology. Optical
42 remote sensing data are an important source of geological information for regional mapping,
43 tectonic structural interpretation of faults, ^{and identification of} large-scale fractures and fracture zones (Suzen and
44 Toprak, 1998; Wladis, 1999; Marghany and Hashim, 2010; Van Der Meer et al., 2012;
45 Hashim et al., 2013).

46 Traditionally, lineament mapping is based on a visual or semi-automatic interpretation of
47 geomorphological features, such as morphotectonic elements, drainage network offsets, and

48 stream segment alignments, and/or spectral criterion, such as tonal changes, patterns and
49 textures.

50 However, the accuracy of features ^{detected} detection from satellite images is affected by several
51 factors including characteristics of the sensor, characteristics of the landform, lighting
52 conditions, and cloud coverage (Smith and Wiseb, 2007). Illumination conditions can be
53 affected by topography: the proportion of light reflected toward the satellite varies with the
54 relative positions of the sun, target, and viewer; the geometry of which varies with topography
55 (Shepherd and Dymond, 2003; Marghany and Hashim, 2010; Rahnama and Gloaguen, 2014).

56 For this reason, the use of a Digital Elevation Model (DEM) or a ^{Digital Terrain Model} (DTM), alone (Simpson and
57 Anders, 1992; Byrd et al., 1994; Collet et al., 2000; Seleem, 2013) or in combination with
58 remotely sensed images on regional scale (Florinsky, 1998; Chorowicz et al., 1999; Jacques et
59 al., 2012), ^{provides} is a useful alternative technique for lineament extraction that avoids most of the
60 limiting factors discussed above (Moore et al., 1991; Jordan et al., 2005; Masoud and Koike,
61 2011). Faults and linear features can be detected and quantified using terrain parameters
62 extracted from a DTM, such as elevation, slope, and convexity (curvature). Morphology
63 characterization is based on slope profiles, curvature values, spatial distribution of
64 homogeneous areas, and cumulative frequency analysis of terrain distribution (Evans, 1980;
65 Jordan et al., 2003; Jordan et al., 2005). For example, curvature maps and slope maps can be
66 used to recognize change in slope gradient, and consequently to identify fault lineaments
67 distribution (Ganas et al., 2005; Jordan et al., 2005). The literature presents several methods
68 based on gridded data of DTMs and DEMs for calculating terrain parameters (Moore at el.,
69 1991; Wise, 2000; Shary et al., 2002; Kienzle, 2004).

70 In this paper, we propose the application of a new semi-automatic approach based on DTMs
71 for the extraction of potential lineaments. The approach tested here was originally developed
72 (Umili et al., 2013) to automatically detect discontinuity traces in rock outcrops to evaluate

73 their degree of fracturing (Umili et al., 2013; Ferrero et al., 2014). In this paper, the method is
74 expanded for feature extraction over a larger area. As a first test area, we selected the
75 Monferrato domain (NW Italy), part of the Tertiary Piedmont Basin (TPB). Significant results
76 have been obtained showing the effectiveness of CurvaTool software for preliminary
77 assessment of potential geological lineaments (Bonetto et al., 2015). Here we further discuss
78 the functionality and applicability of the CurvaTool method in another test area with different
79 accessibility and geological conditions. We selected an area in the Bagni di Vinadio
80 municipality (Cuneo, NW Italy), which is part of the Argentera Massif (Western Alps), as a
81 test ^{area} site to apply the CurvaTool method on a 10 m ground spatial resolution DTM (source
82 Piedmont Region GeoNetwork). We selected this mountainous area for several reasons,
83 including problematic accessibility, interest in the geothermal features of the area, and
84 availability of data from the literature. Data ^{in the test area} obtained from the CurvaTool code (Umili et al.,
85 2013) have been successively compared with literature information and visually extracted
86 lineaments from ortho-photos (Source Arpa Piemonte – data acquisition October 2000).

87

88

89

90 **2 – THE ARGENTERA MASSIF**

91 The Argentera Massif (AM) is in the Western Alps and belongs to the External Crystalline
92 Massifs. It crops out in the footwall of the Penninic Frontal Thrust (Figure 1), and is divided
93 into two main complexes: the Tinée Complex (TC) and the Malinvern-Argentera Complex
94 (MAC), which represent the western and eastern portions of the massif, respectively.

95 **Figure 1 here**

96 The AM is characterized by high grade metamorphic rocks (schist, paragneiss, amphibolites,
97 diatexite and anatectic granitoid), locally intruded by post-metamorphic granitic bodies (Fry,
98 1989; Bogdanoff et al., 2000). The crystalline rocks are unconformably overlain by Triassic to
99 Early Cretaceous carbonates, that are mostly detached above Late Triassic evaporites with the
100 basement-cover contact mainly striking NW-SE (Guglielmetti et al., 2013). ^{The} AM is
101 characterized by Alpine stage ductile shear zones and strike-slip and reverse faults, resulting
102 from brittle reactivations of networks of structures of pre-Alpine and early-Alpine age
103 (Bogdanoff et al., 1991; Musumeci and Colombo, 2002; Corsini et al., 2004; Guglielmetti et
104 al., 2013). Many faults belong to a NW-SE system that mainly consists of right-lateral, high
105 angle, strike-slip faults; a conjugate ^{system} of left-lateral, NE-SW trending ^{faults} system is also present,
106 locally turning to the ENE-WSW (Baietto et al., 2009). In particular, ² three main high angle
107 shear zones cross the AM: the Valletta shear zone (VSZ), the Bersezio fault zone (BFZ) and
108 the Fremamorta shear zone (FMS) (Figure 1). The FMS cuts the center-southernmost portion
109 of the AM, connecting toward north to the BFZ, which consists of a dense set of faults
110 striking NW-SE (Guglielmetti, 2012). The VSZ and the BFZ run parallel to each other in the
111 northern sector of the AM. They are NW-SE oriented and define a 3-km-wide continuous belt
112 ^e made up of high angle strike-slip faults both NW-SE to NNW-SSE and NE-SW to ENE-
113 WSW trending (Baietto et al., 2009; Guglielmetti et al., 2013). The VSZ corresponds to the
114 contact between the TC and MAC, and is represented by an up to one-kilometer-thick
115 mylonitic rock layer formed during a pre-Alpine deformation stage with a dextral strike-slip
116 trend (Musumeci and Colombo, 2002; Guglielmetti et al., 2013). Triassic sedimentary cover
117 unconformably overlies the basement rocks along the Sespoul, La Blance and Tortissa thrusts
118 (Bogdanoff et al., 2000).

119 Seismic and GPS data show that the area is still tectonically active, with crustal shortening of
120 2-4 mm/year induced by N-S to NE-SW compression (Madeddu et al., 1996; Ribolini and
121 Spagnolo, 2008), especially in the axial region of the massif (Perello et al., 2001). The
122 continuing crustal mobility of the Argentera is also indicated by Permanent Scatterers (PS)
123 data (Morelli et al., 2011).

124 The Bagni di Vinadio test area is in the northwestern part of the AM, corresponding with the
125 transition between TC from the west and the MAC from the east (Figure 2). The BFZ and
126 VSZ are the main structures in the area. Migmatitic gneisses, fine-grained aplitic granites, and
127 minor slices of sedimentary rocks mainly occur in the center and south portion of the test
128 area, whereas the sedimentary cover and Permo-Triassic crystalline basement crop out in the
129 northeaster sector of the tested area (Guglielmetti et al., 2013).

130 **Figure 2 here**

131

132

133

134 **3 - METHODOLOGY**

135 We first analyzed the test ^{area} site (Figure 3) by visual detection of linear features, and then with
136 the CurvaTool code (Umili et al., 2013). Results were compared and related to data from the
137 literature. We performed visual lineament extraction on a set of ortho-photos, called "Flight
138 Flood 2000", commissioned by Piedmont Region
139 (http://webgis.arpa.piemonte.it/joomla_gpa_32/) after the flood of October 2000: aerial

140 images (ground spatial resolution of 2.5 m) were collected during autumn 2000 in the north
141 sector of Piedmont and during spring 2001 in its south sector.

142 **Figure 3 here**

143 Visual identification of lineaments is mainly based on the experience of the operator. Two
144 criteria were applied to identify lineaments: (i) geomorphological and (ii) tonality ^{criteria}.
145 Geomorphological criterion is based on the identification of morpho-tectonic and drainage
146 elements, such as rectilinear or segmented patterns of valleys, scarps and ridges, drainage
147 pattern offsets, and stream-segment alignments. Tonality criterion is based on the visual
148 interpretation of differences in color tones and light contrast. Tonality, ^{in fact,} varies as a
149 function of differences in vegetation, lithology, soil water content, permeability, and rock
150 strength (O'Leary et al., 1976). Since the identification of lineaments can be affected by
151 changes in the illumination azimuth and slope, the ortho-photos were enhanced by overlaying
152 the DTM elevation contour map to show the exact location of valleys, ridges, and slope
153 breaks.

154 The CurvaTool code semi-automatic method for lineament identification is based on the
155 assumption that a geological lineament can be geometrically identified as a convex or concave
156 edge ^{of} a DTM, particularly where there is structural control of the geomorphological
157 evolution of the analyzed area. A detailed description of the working principles and
158 calculation methods of CurvaTool code can be found in Bonetto et al. (2015).

159 A DTM (ground resolution of 1 point every 20 m), containing the same area as the one
160 covered by the previously described ortho-photos, was used as input for the CurvaTool code
161 (Umili et al., 2013). Since the area is mountainous, with an elevation difference of 2,130 m,
162 the DTM surface contains a large number of recognizable crests and valleys. ^{Making} Therefore, the
163 area is suitable for semi-automatic linear feature extraction by the CurvaTool code. The code

164 is based on an estimate of principal curvature values (maximum and minimum) associated
165 with each DTM point, thus implementing the method proposed by Chen and Schmitt (1992)
166 and extended by Dong and Wang (2005). As briefly illustrated by the flow chart in Figure 4,
167 the user is asked for two thresholds: [the first one, called] T_{max} , represents the minimum
168 acceptable value of maximum principal curvature (k_{max}) to select DTM points potentially
169 belonging to significant convex edges (e.g. crests); [the second, called] T_{min} , represents the
170 maximum acceptable value of minimum principal curvature (k_{min}) to select DTM points
171 potentially belonging to significant concave edges (e.g. valleys). After a process of points
172 linking, each resulting polyline is segmented: each [obtained] segment is measured and its
173 angle with respect to North [direction is] calculated.

174 **Figure 4 here**

175 The quality of the DTM is fundamental (Kraus, 1993; Kraus and Pfeifer, 1998): the smaller
176 the mean distance between adjacent points, the better the correspondence between the
177 discretized surface and the actual ground surface, and the lower the smoothing effect. The
178 method works particularly well on models with a wide range of principal curvature values,
179 that is on surfaces with a high degree of non-planarity.

180 Once linear feature extraction has been performed, post-processing operations are required in
181 order to obtain significant results; therefore, the algorithm called "Filter" has been [specifically]
182 created by the authors to perform operations on the linear features database (Figure 5). Post-
183 processing can follow two [different] approaches, based on the degree of knowledge of the area
184 and on the purposes of the study. The first approach is applicable in case no literature data are
185 available for the studied area: in this case a frequency analysis is performed on liner features
186 directions; by analyzing the [obtained] ^{resulting} rosette of directions the user can make [considerations] ^{observation}
187 useful for a preliminary tectonic assessment. [In case] ^{where} the area is already geologically well-

188 known and literature data are available for the studied area, in terms of mean direction of
189 lineaments sets, post-processing starts with a comparison with literature data: the user has to
190 assign the minimum lineament length and the orientations of the expected clusters of
191 lineaments (expressed by an angle with respect to the North and its standard deviation). The
192 Filter code deletes linear features shorter than the fixed length and classifies ^{the} each
193 remaining edge, attributing it to the correspondent input cluster. Non-classified features are
194 recorded as "others" (Bonetto et al., 2015). ^{Then,} operations of mapping and statistical
195 analysis of lineaments length can be performed on the obtained database.

then

196 **Figure 5 here**

197

198

199

200 4 – RESULTS AND DISCUSSION

201 A large number of linear features were ^{identified} found in our test area: 1,848 from visual extraction and
202 8,465 by the CurvaTool software (Figure 6). The number of linear features extracted by
203 CurvaTool is remarkable with respect to ^{the number identified by} visual extraction. The 3D geometrical approach
204 implemented in the software allows CurvaTool to identify all concave or convex edges of the
205 ground surface, while visual extraction is subjective and ^{strictly} depends on the experience
206 and ability of the analyst and the observation scale. Moreover, some variations of surface
207 edge are not visually detectable, ^{but} while they can be geometrically described in terms of
208 curvature and therefore analysed by the code.

209 ^{However} On the other hand, a few remarks must be made on the possibility that some of the extracted
210 linear features could be false lineaments, that is natural or artificial linear elements that do not

211 represent geological lineaments. First of all, the ^{DTM} resolution of the DTM plays an important
212 role: in fact, every false lineament whose dimensions are smaller or similar to the ground
213 resolution is not - or only partially- represented by the DTM; therefore it is not detectable as a
214 linear feature by CurvaTool. Considering that a 5 m resolution DTM ^{represents} is already a very detailed
215 model for our purposes, ^{the DTM} this means that it's likely that canals and river banks would not be
216 observable on ^{the DTM} its surface. Moreover, the most common artificial linear elements, such as
217 roads and railroads, are almost flat and therefore, even if detectable on the DTM surface, they
218 belong to areas characterized by non-significant curvature values. However, the possibility
219 that a few linear features representing false lineaments could be detected exists; therefore, a
220 geologically based reasoning must be ^{used} made in this ^{case} sense. Generally, main faults are not
221 isolated structures: the area in which a fault is located is usually characterized by a structural
222 arrangement that reproduces the fault direction. Moreover, our purpose is not only to create a
223 lineament map, but ^{also} is to obtain information about the average direction of lineament sets,
224 ^{instead}. Therefore, a single false lineament cannot invalidate the result of ^a the cluster analysis
225 performed on all ^{the} extracted linear features.
226 Getting back to ^{the} results discussion, all the detected lineaments were statistically analyzed to
227 compare them in terms of quantity, orientation, and geographical distribution.

Unclear what this means

228 **Figure 6 here**

229 Filter was applied to ^{the results of} both the semi-automatic and visual methods to perform a cluster analysis
230 and ^{correctly} assign linear features into ^{different} sets (Bonetto et al., 2015). Four set
231 orientations were assigned, according to geomorphological and structural literature ^{information} [data]
232 (Baietto et al., 2009; Guglielmetti et al., 2013) (Table 1).

233 **Table 1 here**

234 The acronym TELF is assigned to indicate the Total Extracted Linear Features. Using visual
235 extraction (Table 2), NW-SE lineaments (L1) are ^{the least} less frequent (9.42% of TELF), and are
236 mainly in the southern ^{part of the} area; NE-SW lineaments (L2) are the most numerous (19.32% of
237 TELF), and show a principal distribution in the center and south areas. N-S (L3) and E-W
238 lineaments (L4) show a similar frequency (nearly 18% of TELF both for L3 and L4), and are
239 mainly in the northern ^{part of the} area. ^{More than a third of the} (Some) linear features do not correspond to the orientations
240 indicated in Filter: they represent 36% of TELF.

241 **Table 2 here**

242 For the results of the CurvaTool processing (Table 3), the NW-SE set (L1) shows a high
243 frequency (20% of TELF) and uniform distribution in the test area; the NE-SW set (L2) is less
244 frequent (11.79% of TELF) and is chiefly distributed in the center and south-west of the test
245 area. The N-S lineaments (L3) are predominant (20.58% of TELF), and show a homogeneous
246 distribution in the whole area. The E-W set (L4) shows a slightly smaller frequency (20.20 %
247 of TELF), and was mainly identified in the northern and south-eastern ^{parts of the} area. The linear
248 features found with CurvaTool that are not included in the range assigned to Filter represent
249 27% of total features.

250 **Table 3 here**

251 In Figure 7 the different sets have been separated to better compare linear features extracted
252 by visual analysis and ^{CurvaTool} CT processing. Despite the high number of linear features detected, the
253 percentage of unassigned lineaments identified by CurvaTool (27.43%) is lower than that
254 obtained from ^{the} visual ^{method} approach (31.54%). Comparing the percentage of linear features
255 assigned to each set, the main difference between CurvaTool and visual extraction is in the L1
256 and L2 sets (Table 4).

257 **Figure 7 here**

258 **Table 4 here**

259 The sets used in Filter correspond to the orientations of the main geological lineaments in the
260 Argentera Massif; in particular, L1 and L2 correspond to the two main observed conjugate
261 systems that are associated with NW-SE striking thrusts and faults. The NE-SW system (L2)
262 is minor and discontinuous. Set L1 is dominant: it reactivates pre-existing shear zones and
263 pre-alpine foliations in the basement. Also, the basement-cover contact strikes NW-SE
264 (Perello et al., 2001; Baietto et al., 2009). Comparing semi-automatic and visual processing,
265 CurvaTool underestimates the importance of L1, whereas visual extraction overrates L2. This
266 disparity is probably due to the drainage network in the test area, which is [strictly] related to
267 geological lineaments orientation, thus conditioning the detection of linear features. In the test
268 area, most of the main rivers and first order stream channels are NW-SE elongated, and ^{have} show
269 a flat floor. Since ↩
270 DTM points in open valleys correspond to very low and uniform values of curvature, it is
271 likely that they were discarded from the analysis during the choice of curvature thresholds for
272 CurvaTool. The CurvaTool technique is called semi-automatic because the user is asked for
273 two thresholds: minimum and maximum principal curvature values that discriminate between
274 significant and insignificant edges. Therefore, very flat areas are not considered significant for
275 edge identification. However, where the orientation of low-order channels corresponds to a
276 NW-SE strike, both CurvaTool and visual extraction identify linear features belonging to set
277 L1.

278 As reported in Ribolini and Spagnolo (2008), in some portions of the test area, for example
279 along the Stura River, several low-order channels run perpendicular to both the main river
280 stem and geological lineaments [as well]. This type of drainage pattern, where present, could

Thrusts are
faults

281 be the cause of the high number of linear features assigned to L2, particularly by visual
282 extraction where subjectivity and main morphological elements influence the process. Musso
283 et al. (2009) notice that, in the AM, geomorphic evolution is particularly controlled by a NE-
284 SW normal fault system consisting of relatively short segments. Therefore, the influence of
285 morphological criterion on the visual interpretation, is likely the reason for the high
286 percentage of L2 lineaments identified by visual extraction, despite the secondary relevance
287 of this set to L1. Most of the linear features detected by CurvaTool^{0.5} belonging to L1 and L2
288 are short segments aligned along [the] NW-SE and NE-SW directions, respectively. Perello et
289 al. (2001) describes the NW-SE and NE-SW striking systems as discontinuous high angle
290 faults. L3 and L4 have similar percentage values in both [the] analytical approaches. [Field]
291 geological mapping and literature data (Malaroda et al., 1970; Crema et al., 1971; Perello et
292 al., 2001; Baietto et al., 2009; Guglielmetti, 2012), indicate the presence of geological
293 lineaments striking E-W (L4). They are usually short and discontinuous, and frequently
294 connect or displace faults belonging to the main NW-SE system. With regard to the ENE-
295 WSW lineaments, they are associated with the conjugate system of NW-SE strike-slip faults
296 (L2). CurvaTool and visual extraction also detect N-S striking linear features; no important
297 structures with this orientation are known at regional scale in the study area, but detailed field
298 data from Perello et al. (2001) reported the presence of faults with N-S orientation in the
299 Bagni di Vinadio area, associated with low-angle shear zones. Guglielmetti (2012) identified
300 N-S striking morphological elements using photointerpretation, particularly in the SE part of
301 the AM (Terme di Vinadio area).

302 We observed a non-homogeneous distribution of linear features and different lineament
303 domains, particularly using CurvaTool processing (Figure 8). Spatial distribution and
304 alignment of linear features detected by both CurvaTool and visual analysis indicate quite

305 clearly the presence of two main lineaments, in the center and SW part of the test area. When
306 compared to geological mapping data (Malaroda et al., 1970; Crema et al., 1971; Baietto et
307 al., 2009; Guglielmetti, 2012), ^{the two lineament domains} they correspond respectively to the Bersezio and Valletta
308 faults. The anomalous concentration of NW-SE and NE-SW oriented linear features in the
309 middle of these lineaments ^{systems} is due to the presence of ^a the shear zone called ^{the} "Bersezio Fault
310 Zone" (area A in Figure 8 a, b). A change in spatial distribution and frequency of linear
311 features was observed NE of the Stura River. The NE sector (area C in Figure 8 a, b) shows a
312 homogeneous distribution of linear features with preferred NW-SE and E-W orientations,
313 whereas the sector between this domain and the Stura River (area B in Figure 8 a, b) is
314 characterized by a predominance of NE-SW linear features. The boundary between the two
315 sectors seems to correspond to the NW-SE trending basement-cover contact. The south-
316 eastern areas of Bagni di Vinadio town (area D in Figure 8 a, b), bounded on the northwest by
317 the Corborant River, shows a predominance of L4 and L1 features. Part of this sector is
318 geologically still included in the Bersezio ^{fault zone}, a complex system of anastomosing
319 faults made of lens-shape tectonic slices (Perello et al., 2001) formed by NW-SE (L1), NE-
320 SW (L2) and E-W (L4) lineaments. The domain boundaries, particularly as highlighted by
321 CurvaTool, are NW-SE and NE-SW striking, coherent with both main fault directions and
322 iso-kinematic boundaries defined with the PS-InSAR technique by Morelli et al. (2011). Iso-
323 kinematic boundaries are mainly aligned along both a NW-SE direction, parallel or
324 subparallel to the NW-SE transpressive faults, and a NE-SW direction, subparallel to the main
325 drainage network and normal fault system (Musso et al., 2009). In the visual approach, it is
326 possible to observe the same domains, but the above described limits are not as well defined
327 compared to CurvaTool, probably because of the limited number of linear features detected
328 (Figure 8b).

329 **Figure 8 here**

330

331

332

333 **5 - CONCLUSIONS**

334 The CurvaTool code has been applied to DTMs over large areas to semi-automatically detect
335 edges, which represent potential geological linear features. To verify the results obtained by
336 the software, CurvaTool outputs were compared to visually extracted linear features and also
337 to geological literature data.

338 This study ^{demonstrates} shows very well that CurvaTool processing permits extraction and classification of
339 a greater number of linear features compared to visual interpretation. The ability to detect
340 features not perceptible by visual observation is a strong point of CurvaTool processing.
341 Visual interpretation is unable to detect short segments and less evident surface edges as well
342 as CurvaTool; moreover, visual extraction is subjective and influenced by the experience of
343 the analyst. The overall positive aspects of this semi-automatic process include the rapidity of
344 preliminary assessment, the ability to identify the most interesting areas to be investigated,
345 and to analyze areas that are not directly accessible. DTM resolution has a direct influence on
346 lineament definition and completeness. The number of points on the surveyed surface and,
347 consequently, the amplitude of the triangles of the digital model, influence the quality of the
348 approximation of the real surface. In addition, a decrease in resolution results in "smoothing"
349 and consequent deterioration of the edges of the surface. This reduces the range of principal
350 curvatures and, depending on the triangulation, disrupts or alters the continuity of the edges.

351 In the test area, CurvaTool data are consistent with visually detected linear features, and show
352 a good correlation with structural data (Malaroda et al., 1970; Perello et al., 2001; Corsini et
353 al., 2004; Baietto et al., 2009) and iso-kinematic maps (Morelli et al., 2011), demonstrating
354 ^{the applicability} the value of the semi-automatic approach. The abundance of linear features identified by
355 CurvaTool allows for better identification of homogeneous domains (in terms of frequency
356 and distribution of linear features). CurvaTool processing identifies the main faults and shear
357 zones reported in the literature. The alignment of long, single segments and their high density
358 in NW-SE elongated areas, corresponds with the location of the Bersezio and Valletta faults,
359 their deformation zones, and the basement-cover contact.

360 The semi-automatic method has the potential to detect main geomorphic and structural
361 features at a regional scale, particularly in areas where tectonics has a strong control on
362 geomorphic evolution. With regard to the NW sector of the AM, where Bagni di Vinadio is
363 located, the lower relief results in a generally higher sensitivity of the drainage network to
364 faults and fracture systems, which determines preferential orientation of the lineaments
365 (Ribolini and Spagnolo, 2008).

366 Preliminary results of this research show that the application of the CurvaTool code to large
367 areas can be a potential tool in preliminary geological and structural studies, particularly in
368 areas that are not directly accessible or when scarce existing data are available. CurvaTool can
369 give useful and rapid information about the orientation and spatial distribution of potential
370 geological and geomorphological lineaments, and the possible presence of domains with
371 homogeneous features and lineament distributions. Based on this approach, further specific
372 field studies can be planned to verify these results.

373 In alpine environments, CurvaTool shows a high potential due to less ^{quaternary} cover
374 obscuring tectonic elements, and it is easier to validate results because of the abundance of
375 outcrops and field data. Further research in the test area will consist of statistical analysis of

376 the frequency distribution and length of the lineaments belonging to each set, and the
377 influence of rock type on the linear feature detection. Subsequent investigations and statistical
378 processing of the data are needed to validate and improve the software. Additionally, testing
379 new areas with different tectonic and geomorphologic environments is also a future priority.

380

381

382

383 REFERENCES

384 ✓ Baietto, A.; Perello, P.; Cadoppi, P.; and Martinotti, G., 2009, Alpine tectonic evolution and
385 thermal water circulations of the Argentera Massif (South-western Alps): *Swiss Journal*
386 *Geosciences*, Vol. 102, pp. 223–245.

387 ✓ Bogdanoff, S.; Michard, A.; Mansour, M.; and Poupeau, G., 2000, Apatite fission tracks
388 analysis in the Argentera massif: evidence of contrasting denudation rates in the external
389 crystalline massifs of the Western Alps: *Terra Nova*, Vol. 12, pp. 117–125.

390 ✓ Bogdanoff, S.; Menot, R.; and Viviner, G., 1991, Les massifs cristallins externes des Alpes
391 Occidentales francaises, un fragment de la zone interne varisque: *Science Geologique*
392 *Bullettin*, Vol. 44, pp. 237–285.

393 ✓ Bonetto, S.; Facello, A.; Ferrero, A. M.; and Umili, G., 2015, A tool for semi-automatic linear
394 feature detection based on DTM: *Computers & Geosciences*, Vol. 75, pp. 1–12.

395 ✓ Byrd, J. O. D.; Smith, R. B.; and Geissman, J. W., 1994, The Teton fault, Wyoming:
396 neotectonics, and mechanisms of deformation: *Journal Geophysical Research*, Vol 99 (B10),
397 pp. 20095–20122.

- 398 ✓Chen, X. and Schmitt, F., 1992, Intrinsic surface properties from surface triangulation:
399 Springer Berlin Heidelberg (Editor) *European Conference on Computer Vision*, pp. 739-743.
- 400 ✓Chorowicz, J.; Dhont, D.; and Gundogdu, N., 1999, Neotectonics in the eastern North
401 Anatolian fault region (Turkey) advocates crustal extension: mapping from SAR ERS
402 imagery and Digital Elevation Model: *Journal Structural Geology*, Vol. 21, pp. 511–532.
- 403 ✓Clark, C. D.; and Wilson, C., 1994, Spatial analysis of lineaments: *Computers & Geosciences*,
404 Vol. 20 (7-8), pp. 1237–1258.
- 405 ✓Collet, B.; Taud, H.; Parrot, J. F.; Bonavia, F.; and Chorowicz, J., 2000, A new kinematic
406 approach for the Danakil block using a Digital Elevation Model representation:
407 *Tectonophysics*, Vol. 316, pp. 343–357.
- 408 ✓Corsini, M.; Ruffet, G.; and Caby, R., 2004, Alpine and late-hercynian geochronological
409 constraints in the Argentera Massif (Western Alps): *Eclogae Geologicae Helvetiae*, Vol. 97,
410 pp. 3–15.
- 411 ✓Crema G.; Dal Piaz G.; Merlo C.; and Zanella E., 1971, Carta geologica d'Italia alla scala
412 1:100.000, Fogli Argentera, Dronero, Demonte, n. 78, 79 e 90 e Note illustrative: *Istituto*
413 *Poligrafico e Zecca dello Stato - Archivi di Stato*, Roma [in Italian].
- 414 ✓Davis, G. H. and Reynolds, S. J., 1996, *Structural geology of rocks and regions*: John Wiley
415 & Sons, New York, 2nd Ed.
- 416 ✓Dong, C. and Wang, G., 2005, Curvatures estimation on triangular mesh: *Journal Zhejiang*
417 *University Science*, Vol.6A (Suppl I), pp. 128-136.
- 418 ✓Evans, I. S., 1980, An integrated system of terrain analysis and slope mapping: *Zeitschrift*
419 *Geomorphologie*, Vol. 36, pp. 274-295.

- 420 ✓ Ferrero A. M., Migliazza M. R. and Umili G., 2014, Rock mass characterization by means of
421 advanced survey methods. Keynote lecture. Rock Engineering and Rock Mechanics:
422 Structures in and on Rock Masses: *Proceedings of EUROCK 2014, ISRM European Regional*
423 *Symposium*, Vigo, Spain, 27-29 May 2014, pp. 17-27, ISBN 978-1-138-00149-7.
- 424 ✓ Florinsky, I. V., 1998, Combined analysis of digital terrain models and remotely sensed data
425 in landscape investigations: *Progress Physical Geography*, Vol. 22, pp. 33–60.
- 426 ✓ Fry, N., 1989, Southwestward thrusting and tectonics of the western Alps. In: Coward, M. P.,
427 Dietrich, D., Park, R. G. (Editors.), *Alpine Tectonics: Geological Society of London, Special*
428 *Publication*. Vol. 45, pp. 83–109.
- 429 ✓ Ganas, A.; Pavlides, S.; and Karastathis, V., 2005, DEM-based morphometry of range-front
430 escarpments in Attica, central Greece, and its relation to fault slip rates: *Geomorphology*, Vol.
431 65, No. 3, pp. 301-319.
- 432 ✓ Guglielmetti L.; Comina C.; Abdelfettaha Y.; Schill E.; and Mandrone G., 2013, Integration
433 of 3D geological modeling and gravity surveys for geothermal prospection in an Alpine
434 region: *Tectonophysics*, Vol. 608, pp. 1025–1036.
- 435 ✓ Guglielmetti, L., 2012. *Multidisciplinary Approach of Geothermal Exploration in the*
436 *Argentera Massif (Southwestern Alps)*: PhD Thesis, Department of Earth Sciences, Torino
437 University, Italy, 193 p.
- 438 ✓ Hashim, M.; Ahmad, S.; Johari, M. A. M.; and Pour, A. B., 2013, Automatic lineament
439 extraction in a heavily vegetated region using Landsat Enhanced Thematic Mapper (ETM+)
440 imagery: *Advances Space Research*, Vol. 51, No. 5, pp. 874–890.

- 441 ✓ Jacques, P. D.; Machado, R.; and Nummer, A. R., 2012, A comparison for a multiscale study
442 of structural lineaments in southern Brazil: LANDSAT-7 ETM+ and shaded relief images
443 from SRTM3-DEM: *Anais Academia Brasileira Ciências*, Vol. 84, No. 4, pp. 931-942.
- 444 ✓ Jordan G.; Meijninger B. M. L.; van Hinsbergen D. J. J.; Meulenkamp J. E.; and van Dijk P.
445 M., 2005, Extraction of morphotectonic features from DEMs: development and applications
446 for study areas in Hungary and NW Greece: *International Journal Applied Earth Observation*
447 *Geoinformation*, Vol. 7, pp. 163–182.
- 448 ✓ Jordan, G.; Csillag, G.; Szucs, A.; and Qvarfort, U., 2003, Application of digital terrain
449 modelling and GIS methods for the morphotectonic investigation of the Kali Basin, Hungary:
450 *Zeitschrift Geomorphologie*, Vol. 47, pp. 145 - 169.
- 451 ✓ Kienzle, S., 2004, The effect of DEM raster resolution on first order, second order and
452 compound terrain derivatives: *Transactions GIS*, Vol. 8, No. 1, pp. 83-111.
- 453 ✓ Kraus, K., 1993, *Photogrammetry, vol 1*, 4th ed.: Dummler, F. (Editor), Bonn. ISBN:3-427-
454 78684-6.
- 455 ✓ Kraus, K.,^{and} Pfeifer, N., 1998, Determination of terrain models in wooded areas with airborne
456 laser scanner data: *ISPRS Journal Photogrammetry & Remote Sensing*, Vol. 53, No. 4, pp.
457 193–203.
- 458 ✓ Lee, M.; Morris, W.; Harris, J.; and Leblanc, G., 2012, An automatic network-extraction
459 algorithm applied to magnetic survey data for the identification and extraction of geologic
460 lineaments: *Leading Edge*, Vol. 31, No. 1, pp. 26–31.

- 461 ✓ Madeddu, B.; Bertoux, N.; and Stephan, J. F., 1996, Champ de contrainte post-pliocene et
462 deformation recentes dans les Alpes sud-occidentales: *Bulletin Societe Geologique France*,
463 Vol. 8, pp. 797–810.
- 464 ✓ Malaroda, R.; Carraro, F.; Dal Piaz, G. B.; Franceschetti, B.; Sturani, C.; and Zanella, E.,
465 1970, Carta Geologica del Massiccio dell'Argentera alla scala 1:50.000 e Note Illustrative:
466 *Memorie Società Geologica Italiana*, Vol. 9, pp. 557–663 [in Italian].
- 467 ✓ Marghany, M.; and Hashim, M. 2010, Lineament mapping using multispectral remote sensing
468 satellite data research: *Journal Applied Sciences*, Vol. 5, No. 2, pp. 126-130.
- 469 ✓ Masoud, A.; and Koike, K., 2011, Morphotectonics inferred from the analysis of topographic
470 lineaments autodetected from DMEs: application and validation for the Sinai Peninsula,
471 Egypt: *Tectonophysics*, Vol. 510, pp. 291–308.
- ✓472 Moore, I. D.; Grayson, R. B.; and Ladson, A. R., 1991, Digital terrain modelling: a review of
473 hydrological, geomorphological, and biological applications: *Hydrological processes*, Vol. 5,
474 No. 1, pp. 3-30.
- 475 ✓ Morelli, M.; Piana, F.; Mallen, L.; Nicolò, G.; and Fioraso, G., 2011, Iso-kinematic maps
476 from statistical analysis of PS-InSAR data of Piemonte, NW Italy: comparison with
477 geological kinematic trends: *Remote Sensing Environment*, Vol. 115, No. 5, pp. 1188–1201.
- 478 ✓ Musso, A.; Piana, F.; Bertok, C.; d'Atri, A.; Martire, L.; Perotti, E.; and Varrone, D., 2009,
479 Post-eocene transpression in Western Ligurian Alps: Geometry and kinematics of Limone-
480 Viozene Deformation Zone (France-Italy border): *Epitome*, Vol. 3, pp. 181.

- 481 ✓ Musumeci, G.; and Colombo, F., 2002, Late Visean mylonitic granitoids in the Argentera
482 Massif (western Alps, Italy): age and kinematic constraints on the Ferriere–Mollieres shear
483 zone: *Comptes Rendus Geoscience*, Vol. 334, pp. 213–220.
- 484 ✓ O’Leary, D. W.; Friedman, J. D.; and Pohn, H. A., 1976, Lineament, linear, lineation: some
485 proposed new standards for old terms: *Geological Society America Bulletin*, Vol. 87, No. 10,
486 pp. 1463–1469.
- 487 ✓ Perello, P.; Marini, L.; Martinotti, G.; and Hunziker, C., 2001, The thermal circuits of the
488 Argentera Massif (western Alps, Italy): an example of low enthalpy geothermal resources
489 controlled by Neogene alpine tectonics: *Eclogae Geologicae Helvetiae*, Vol. 94, pp. 75–94.
- 490 ✓ Rahnama, M.; and Gloaguen, R., 2014, TecLines: a MATLAB-based toolbox for tectonic
491 lineament analysis from satellite images and DEMs, part 1: Line segment detection and
492 extraction: *Remote Sensing*, Vol. 6, No. 7, pp. 5938–5958.
- 493 ✓ Rangzan, K.; Charchi, A.; Abshirini, E.; and Dinger, J., 2008, Remote sensing and GIS
494 approach for water-well site selection, southwest Iran: *Environmental & Engineering*
495 *Geoscience*, Vol. 14, pp. 315–326.
- 496 ✓ Ribolini, A.; and Spagnolo, M., 2008, Drainage network geometry versus tectonics in the
497 Argentera Massif (French–Italian Alps): *Geomorphology*, Vol. 93, pp. 253–266.
- 498 ✓ Shary, P. A.; Sharaya, L. S.; and Mitusov, A. V., 2002, Fundamental quantitative methods of
499 land surface analysis: *Geoderma*, Vol. 107, No. 1, pp. 1-32.
- 500 ✓ Seleem T. A., 2013, Analysis and tectonic implication of DEM-derived structural lineaments,
501 Sinai Peninsula, Egypt: *International Journal Geosciences*, Vol. 4, pp. 183-201.

502 ✓ Shepherd, J. D.; and Dymond, J. R., 2003, Correcting satellite imagery for the variance of
503 reflectance and illumination with topography: *International Journal Remote Sensing*, Vol. 24,
504 No. 17, pp. 3503–3514.

505 ✓ Simpson, D. W.; and Anders, M. H., 1992, Tectonics and topography of the Western United
506 States - an application of digital mapping: *GSA Today*, Vol. 2, No. 6, pp. 117–121.

507 ✓ Smith, M. J.; and Wiseb, S. M., 2007, Problems of bias in mapping linear landforms from
508 satellite imagery: *International Journal Applied Earth Observation Geoinformation*, Vol. 9,
509 pp. 65–78.

510 ✓ Suzen, M. L.; and Toprak, V., 1998, Filtering of satellite images in geological lineament
511 analyses: an application to a fault zone in Central Turkey: *International Journal of Remote*
512 *Sensing*, Vol. 19, No. 6, pp. 1101–1114.

513 ✓ Umili, G.; Ferrero, A. M.; and Einstein, H. H., 2013, A new method for automatic
514 discontinuity traces sampling on rock mass 3D model: *Computers & Geosciences*, Vol. 51,
515 pp. 182–192.

516 ✓ Van der Meer, F. D.; Van der Werff, H. M. A.; Van Ruitenbeek, F. J. A.; Hecker, C. A.;
517 Bakker, W. H.; Noomen, M. F.; Van der Meijde, M.; Carranza, E. J. M.; Boudewijn de
518 Smeth, J.; and Woldai, T., 2012, Multi- and hyperspectral geologic remote sensing: A review:
519 *International Journal Applied Earth Observation Geoinformation*, Vol. 14, No. 1, pp. 112-
520 128.

521 ✓ Wise, S., 2000, Assessing the quality for hydrological applications of digital elevation models
522 derived from contours: *Hydrological Processes*, Vol. 14, No. 11-12, pp. 1909-1929.

523 Wladis, D., 1999, Automatic lineament detection using digital elevation models with second
524 derivative filters: *Photogrammetric Engineering & Remote Sensing*, Vol. 65, No. 4, pp. 453–
525 458.

526

527

528

529 **List of Tables:**

530 Table 1 – Orientation of lineament sets used as input for Filter.

531

532 Table 2 – Statistics for visually extracted lineaments.

533

534 Table 3 – Statistics for lineaments obtained from CurvaTool processing.

535

536 Table 4 – Comparison between classified lineaments obtained from CurvaTool processing and

537 visual interpretation.

538

539 **List of Figures:**

540

541 Figure 1 - Tectonic sketch map of the Argentera Massif and adjoining regions. BFZ: Bersezio

542 fault zone, BF: Bersezio fault, VSZ: Valletta shear zone, FMS: Fremamorta shear zone.

543 (source: Baietto et al., 2009). The box highlights the investigated area.

544

545 Figure 2 - Geological map of Bagni di Vinadio area (source: Guglielmetti et al., 2013).

Too small to
be legible - enlarge
to full page size.

546

547 Figure 3 – Test area: Bagni di Vinadio, Argentera Massif. Base map: orto-photo Flight Flood
548 2000 (source: Arpa Piemonte)

549

550 Figure 4 – Flow chart representing CurvaTool process

551

552 Figure 5 – Flow chart representing Filter process

— figure blanked out.

553

554 Figure 6- Maps of lineaments of Bagni di Vinadio obtained from visual extraction (a) and by
555 CurvaTool processing (b).

Figure 6a partially blanked out

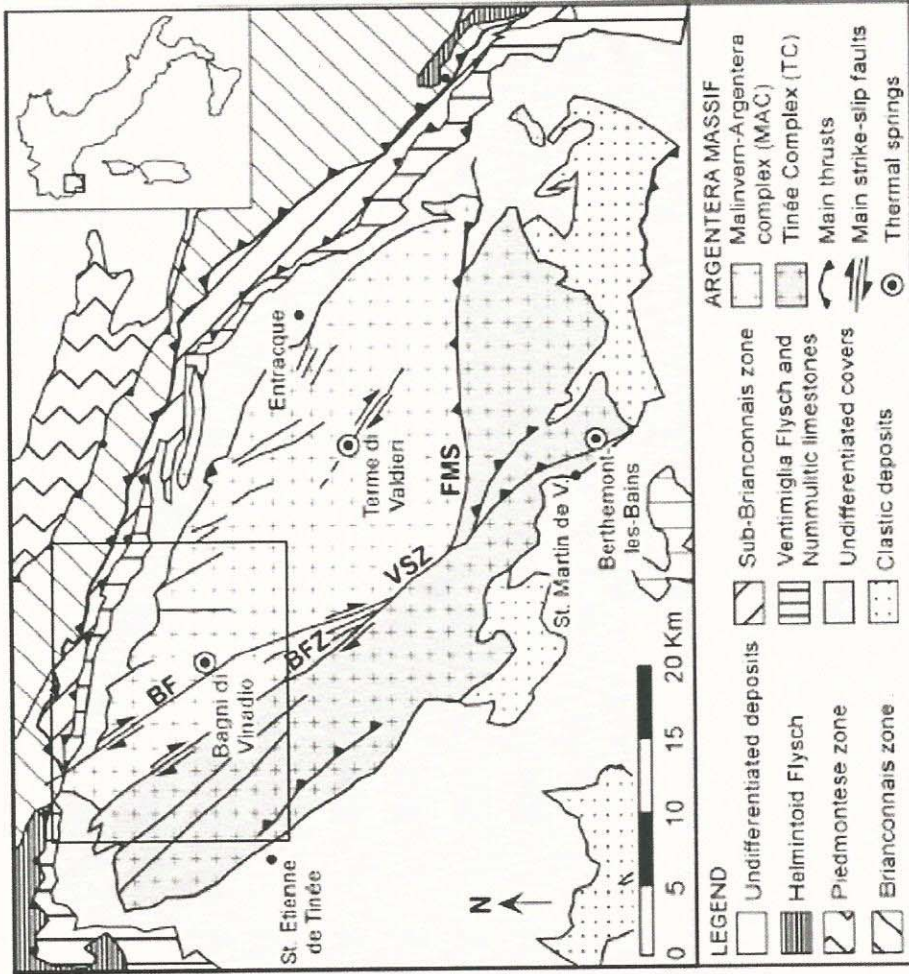
556

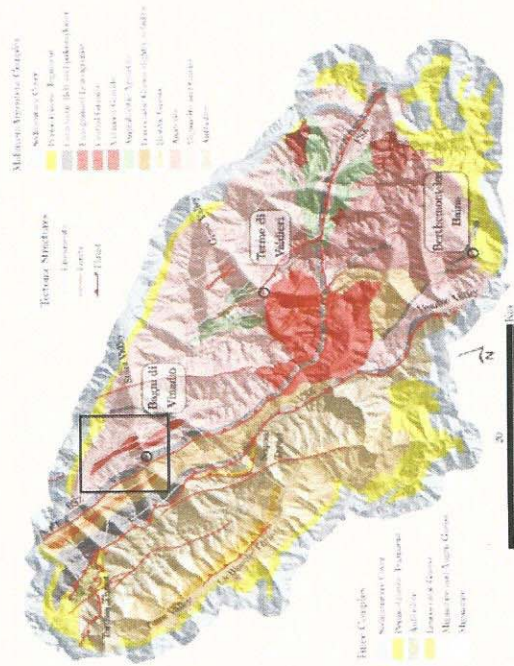
557 Figure 7- Map of linear features of Bagni di Vinadio extracted and processed with Filter. Four
558 sets are highlighted: (a) L1 (NW-SE), (b) L2 (NE-SW), (c) L3 (N-S) and (d) L4 (E-W).

— obscured

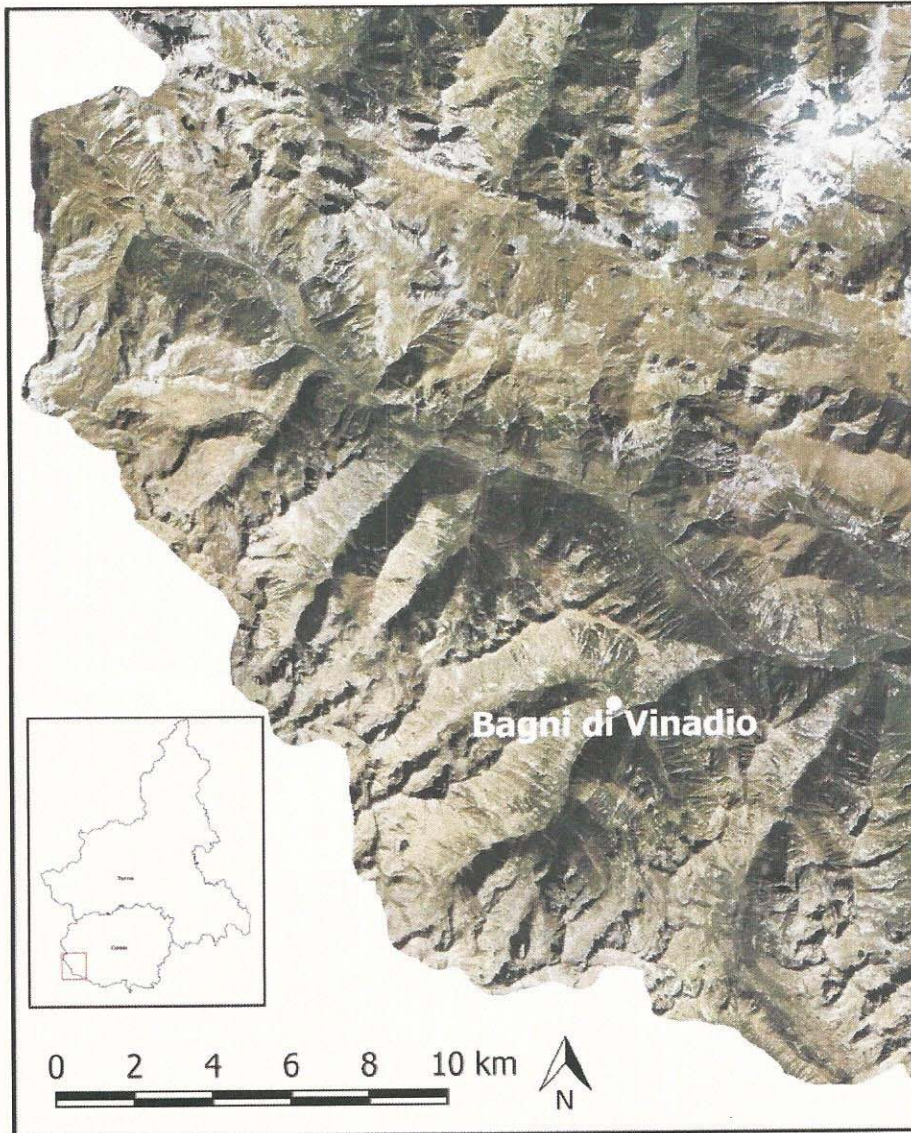
559

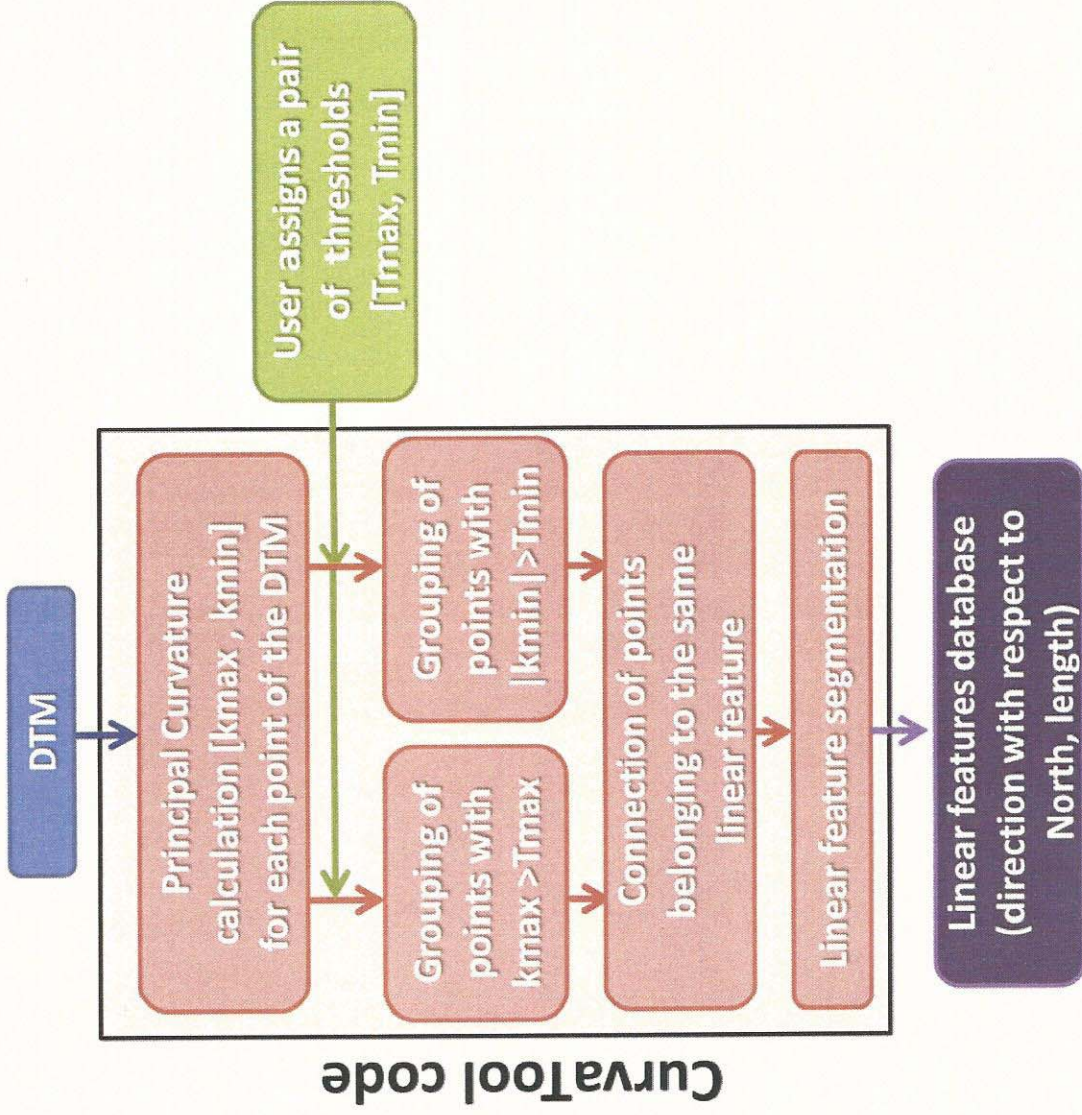
560 Figure 8 - Main geological lineaments obtained by (a) visual extraction and (b) CurvaTool,
561 and then processed with Filter. Areas characterized by an homogeneous/specific linear feature
562 distribution are indicated as domains A, B, C, D.





100 small-male full page size.



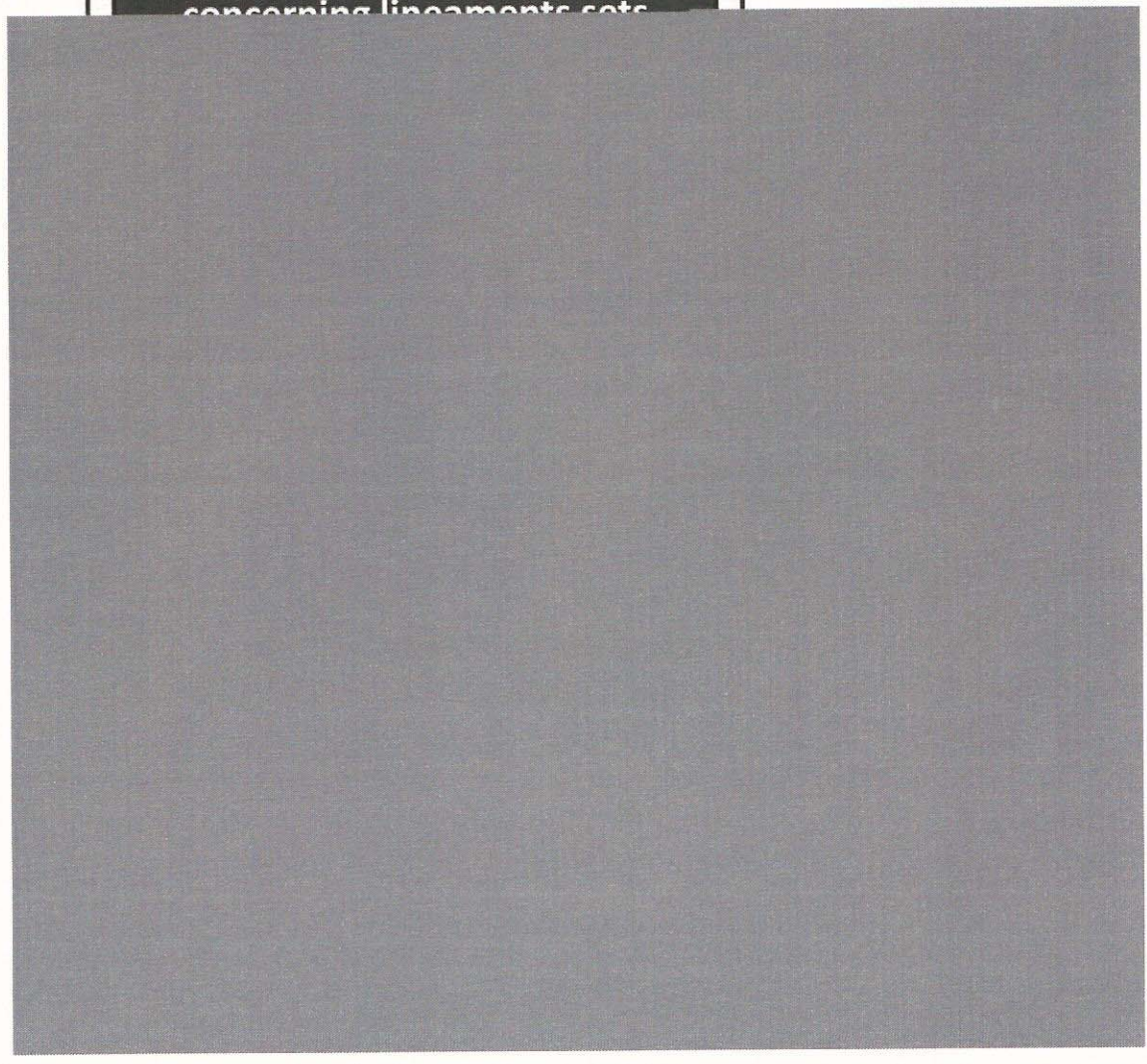


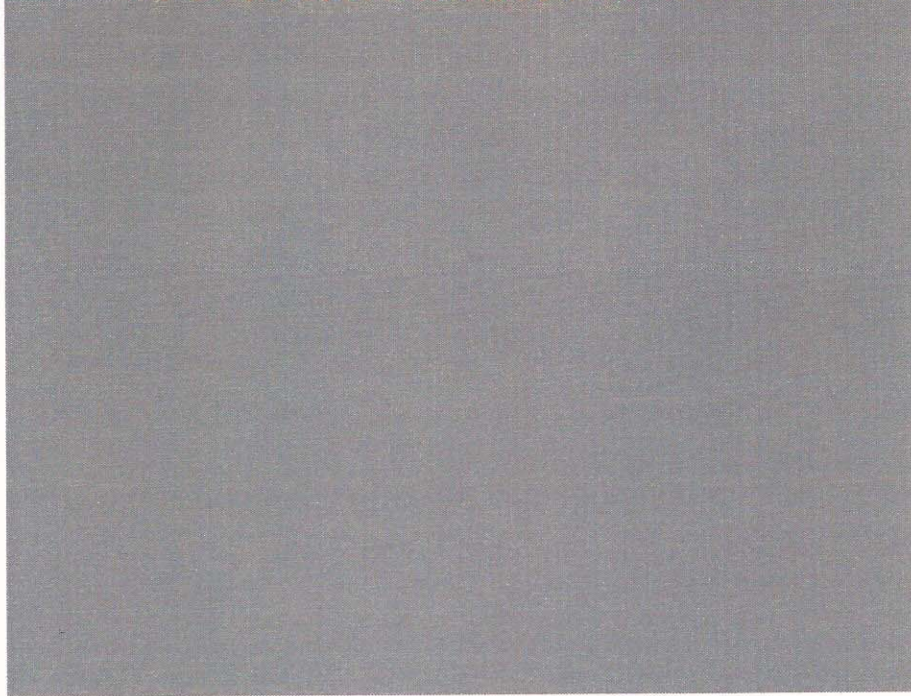
Linear features database



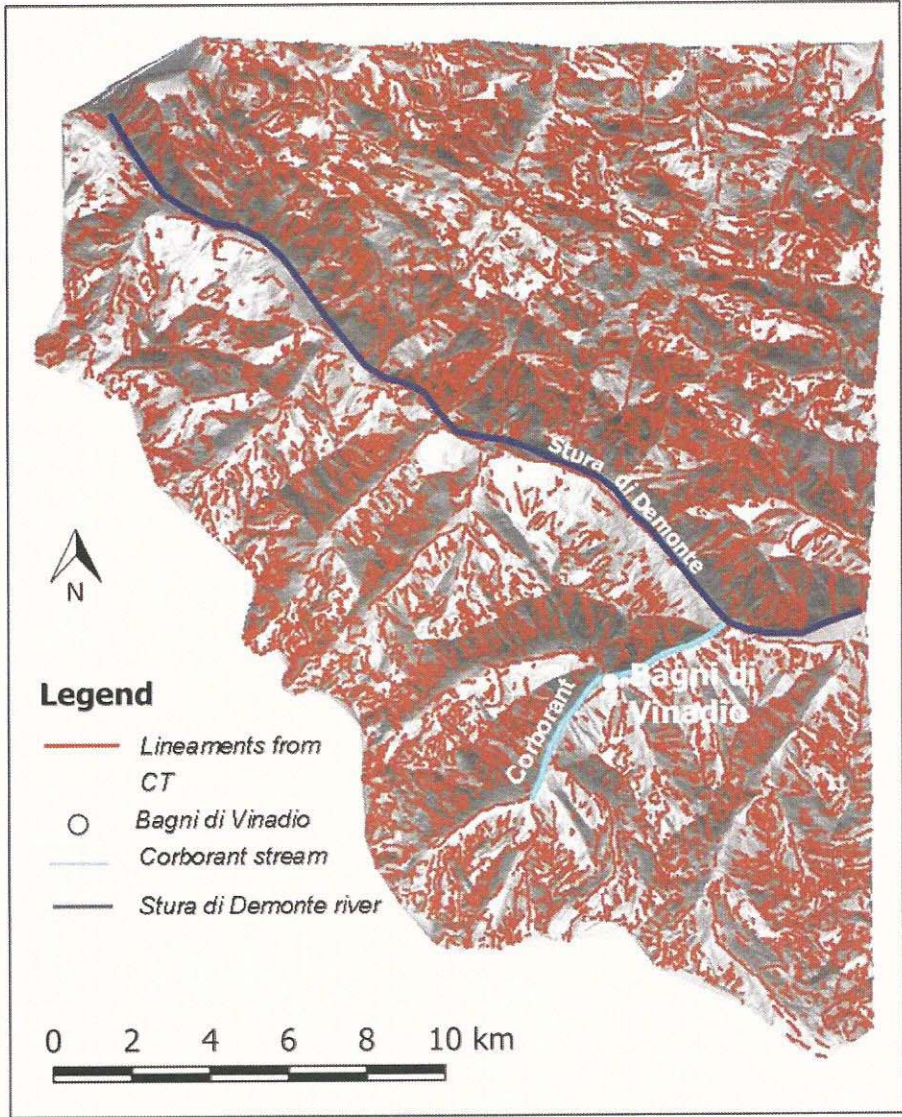
Available literature data
concerning lineaments sets

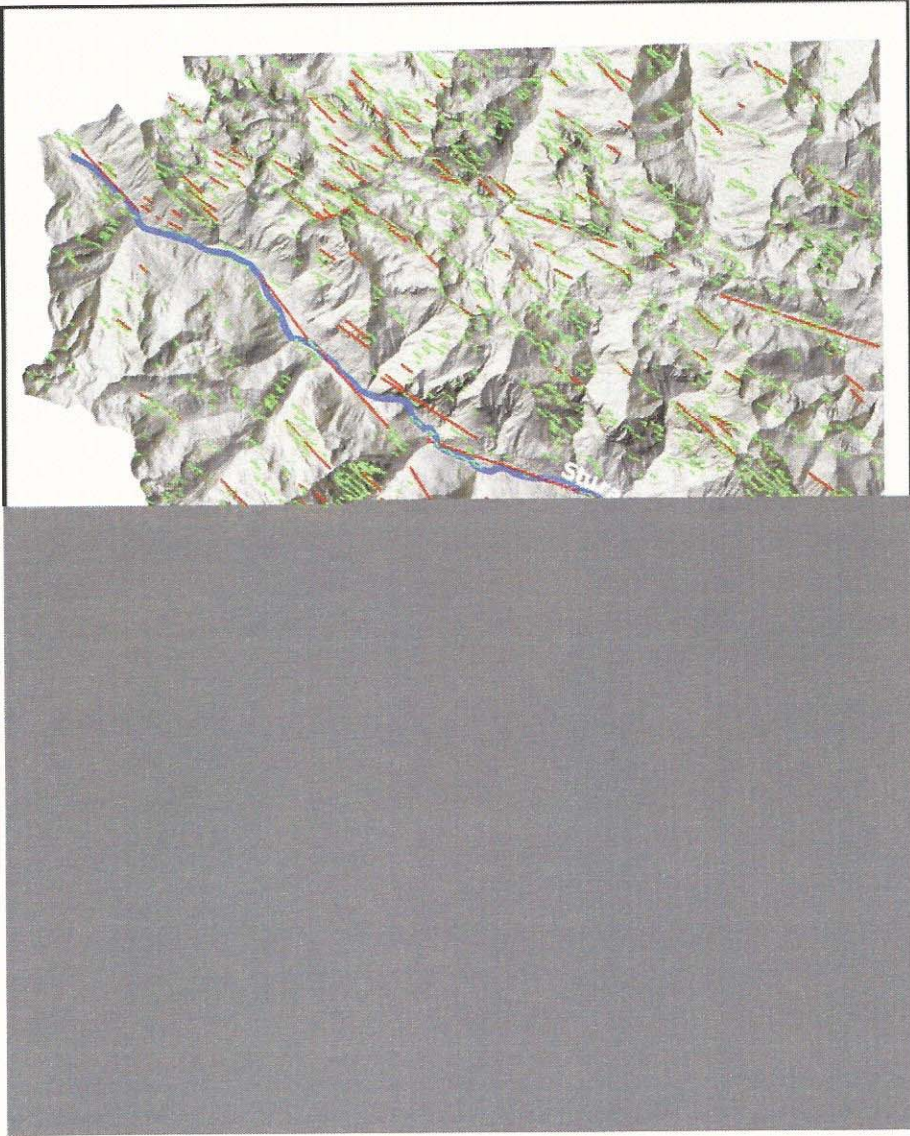
A
/

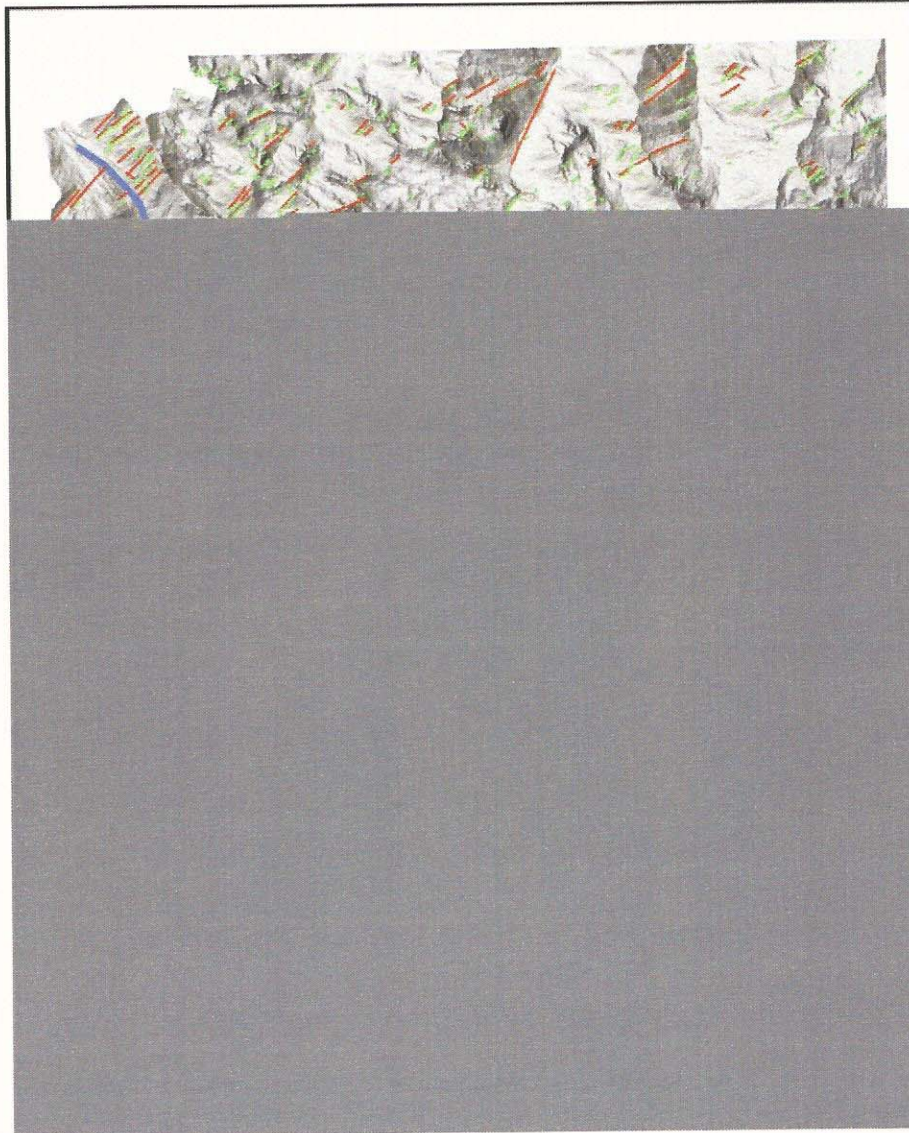


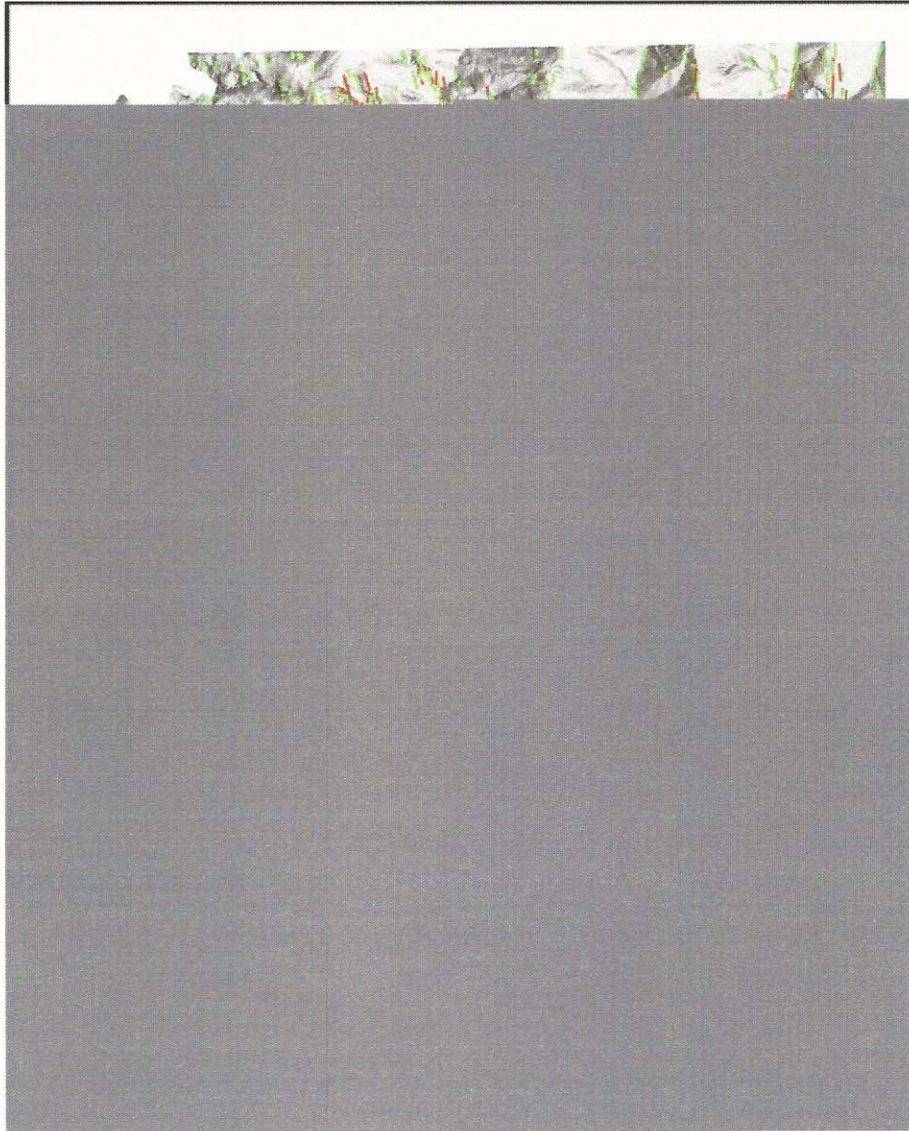


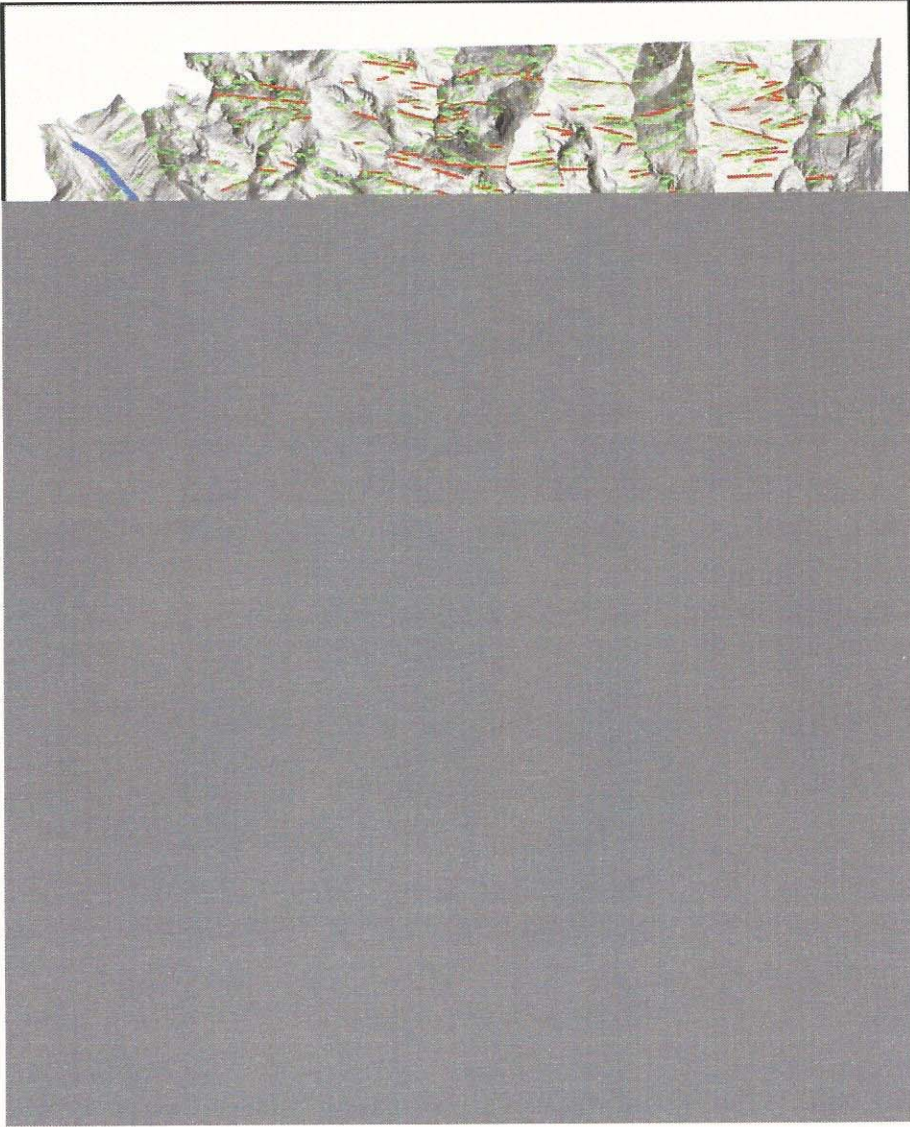
?

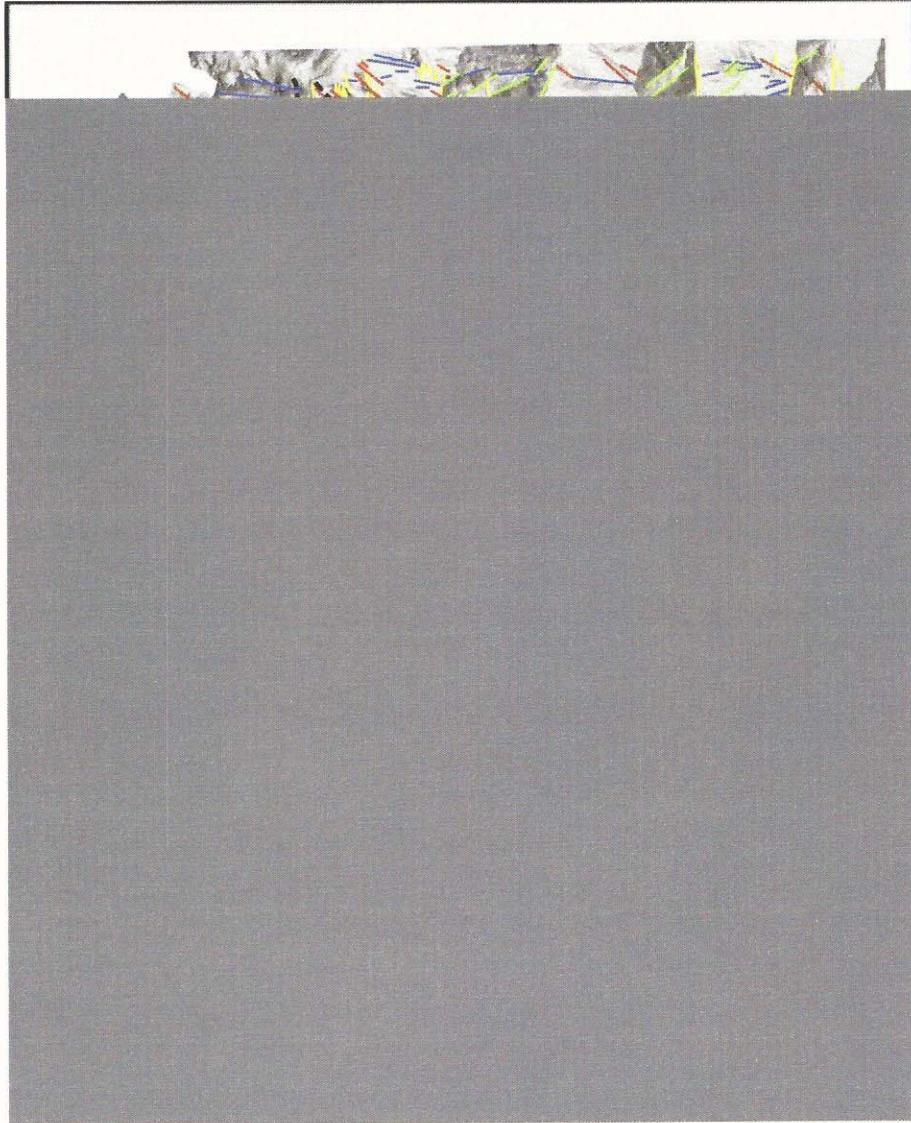












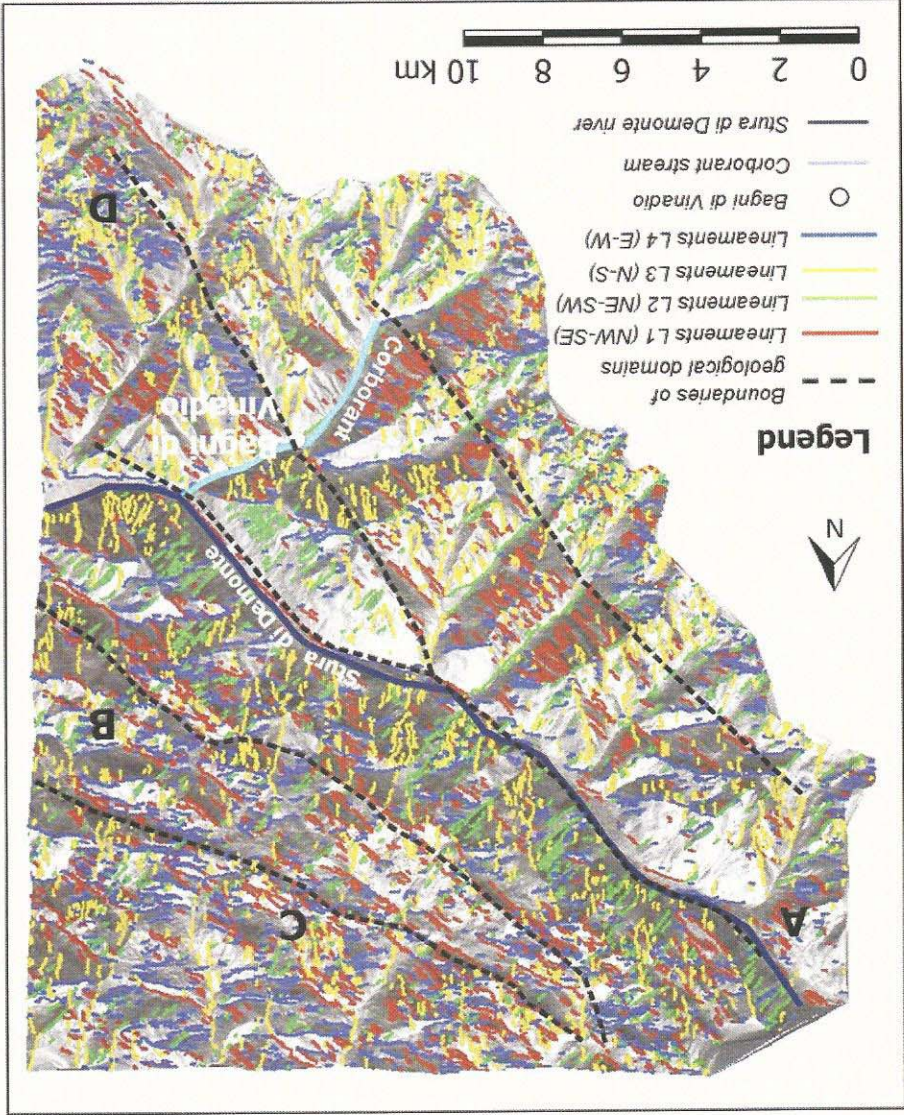


Table 1 – Orientation of lineament sets used as input for Filter.

Set	Azimuthal Direction [deg]	Standard Deviation [deg]
L1	N125	15
L2	N50	10
L3	N0	20
L4	N90	19.99

Table 2 –Statistics for visually extracted lineaments.

Set	n° Lineaments	Azimuthal Direction [deg]			
		Minimum	Maximum	Mean	Standard Deviation
L1	174	110.05	139.90	124.85	8.39
L2	357	40.24	59.86	49.38	5.36
L3	331	0.00	19.98	0.23	11.12
L4	329	70.02	109.98	87.56	10.62

Table 3 – Statistics for lineaments obtained from CurvaTool processing.

Set	n° Lineaments	Azimuthal Direction [deg]			
		Minimum	Maximum	Mean	Standard Deviation
L1	1693	110.10	139.99	126.66	8.36
L2	998	40.10	59.94	49.77	5.65
L3	1742	-19.98	19.98	-0.89	11.76
L4	1710	70.02	109.98	90.43	11.59

Table 4 – Comparison between classified lineaments obtained from CurvaTool processing and visual interpretation.

Set	Percentage of total linear features (8465) extracted by CurvaTool	Percentage of total linear features (1883) visually extracted
L1	20.00%	11.78%
L2	11.79%	21.93%
L3	20.58%	17.57%
L4	20.20%	17.15%
Not Assigned	27.43%	31.54%